Shedding Light On Blue-Green Photosynthesis: A Wavelength-Dependent Mathematical Model Of Photosynthesis In *Synechocystis* sp. PCC 6803

Tobias Pfennig[a,b,1], Elena Kullmann[a], Tomáš Zavřel[c], Andreas Nakielski[a,d], Oliver Ebenhöh[b,e], Jan Červený[c], Gábor Bernát[f], and Anna Matuszyńska[a,b]

[a]Computational Life Science, Department of Biology, RWTH Aachen University, 52074 Aachen, Germany
[b]Cluster of Excellence on Plant Science, Heinrich Heine University (HHU) Düsseldorf, Germany
[c]Department of Adaptive Biotechnologies, Global Change Research Institute, Czech Academy of Sciences, Brno, Czechia
[d]Institute for Synthetic Microbiology, HHU Düsseldorf, 40225 Düsseldorf, Germany
[e]Institute of Theoretical and Quantitative Biology, HHU Düsseldorf, 40225 Düsseldorf, Germany
[f]Balaton Limnological Research Institute, Eötvös Loránd Research Network (ELKH), Tihany, Hungary
[1]To whom correspondence should be addressed. E-mail: tobias.pfennig@rwth-aachen.de

Abstract

Cyanobacteria hold great potential to revolutionize conventional industries and farming practices with their light-driven chemical production. To fully exploit their photosynthetic capacity and enhance product yield, it is crucial to investigate their intricate interplay with the environment, in a particular light. Mathematical models provide valuable insights for optimising strategies in this pursuit. In this study, we present an ordinary differential equation-based model for cyanobacterium *Synechocystis* sp. PCC 6803 to assess its performance under various light sources, including monochromatic light. Our model accurately predicts the partitioning of electrons through four main pathways, O_2 evolution, and the rate of carbon fixation. Additionally, it successfully captures chlorophyll fluorescence signals, enabling valuable information extraction. We explore state transition mechanisms, favouring PSII quenching over PBS detachment based on theoretical evidence. Moreover, we evaluate metabolic control for biotechnological production under diverse light colours and irradiances. By offering a comprehensive computational model of cyanobacterial photosynthesis, our work enhances understanding of light-dependent cyanobacterial behaviour and supports optimising their metabolism for industrial applications.

Keywords: cyanobacteria | light spectrum | mathematical model | photosynthesis | state transitions.

Cyanobacteria are responsible for a quarter of global carbon fixation [1]. They are, in fact, the originators of oxygenic photosynthesis, later transferring this capability to other organisms via endosymbiosis [2]. Despite their relative simplicity in cellular structure, the cyanobacterial photosynthetic machinery is a highly sophisticated system that shows significant differences from their plastidic relatives. Recently, they have emerged as a powerful resource for research and biotechnology due to their unique combination of beneficial traits and photosynthetic capabilities [3]. In the quest for environmentally friendly alternatives to fossil fuels and sugar-based production, cyanobacteria stand out as promising candidates due to their ability to convert sunlight and CO_2 into valuable products, their minimal growth re-

quirements, and their adaptability to diverse environments. Their metabolic versatility allows for producing a wide range of biofuels, chemicals, and raw materials. Besides biomass [4], the cells can be harvested for a variety of primary and secondary metabolites, such as sugars and alcohols [5, 6], chlorophyll and carotenoids [3], (poly)peptides and human vitamins [7], and terpenoids [8]. In particular, strains of the model cyanobacteria *Synechocystis* sp. PCC 6803 and *Synechococcus elongatus* PCC 7942, are highly attractive platform organisms for the phototrophic production of e.g. isoprene, squalene, valencene, cycloartenol, lupeol or bisabolene [8]. Leveraging the cells' natural capabilities, isolation of molecular hydrogen [9] and reduced nitrogen [3] is also possible, with uses in energy and agronomic sectors. Furthermore, there have been attempts to use cyanobacteria for bioelectricity production [10, 6] or, inversely, to overcome cellular limitations by fuelling cyanobacteria with induced electrical currents [11].

The basis of photosynthesis and distinction to plant research

Compared to plants, the prokaryotic cell structure differs crucially. The cells are ca. 100x smaller (~15 fL; [12]) and lack principal plant cell components like organelles [13]. Consequently, cyanobacterial thylakoids, the membrane-bound compartments hosting the photosynthetic machinery, are located within the cytoplasm. Furthermore, while cyanobacteria and chloroplasts share a common ancestry and possess fundamentally similar photosynthetic systems, there are many differences at the level of proteins and reactions [14, 15]. For example, cyanobacteria can perform photosynthesis and respiration, allowing for auto-, hetero-, and mixotrophic lifestyles [15]. But, due to the lack of mitochondria, cyanobacteria perform respiration within the same membrane, sharing some of the electron carriers and proteins within the Photosynthetic Electron Transport Chain (PETC) [10]. Hence, photosynthetic and Respiratory Electron Transport (RET) are strongly linked. Additionally, several non-linear alternative electron flows adapt the cell to different light conditions or metabolic demands (Cyclic Electron Transport (CET) and Water-Water Cycle (WWC)). Although the PETC is largely composed of protein complexes similar to those in plants, the light-absorbing complexes in cyanobacteria are hugely different. The cyanobacterial light-harvesting antennae (Phycobilisomes (PBSs)) and photoprotection mechanism (the Orange Carotenoid Protein (OCP)) do not exist *in plantae*. Therefore, light-based measuring techniques like Pulse Amplitude Modulation (PAM) fluorescence, a non-invasive method developed for plant research [16] may require adapting protocols or interpretation [17]. Compared to plants and green algae, cyanobacterial PAM-measured fluorescence has contributions from PSII, PSI, and detached PBS resulting in distinct fluorescence behaviour [18].

While photosynthesis and respiration represent the source of energy and redox equivalents, other pathways serve as the cell's sink reactions. The Calvin-Benson-Bassham cycle (CBB) is most significant in these autotroph organisms as it uses ATP and NADPH to fix CO_2 into 3-phosphoglycerate (3PGA) to produce all organic metabolites [10]. However, Ribulose-1,5-bisphosphate Carboxylase-Oxygenase (RuBisCO), the CBB's primary enzyme for fixing CO_2, may also react with O_2, producing cytotoxic 2-phosphoglycolate (2PG) in the process. Including the following costly detoxification, this Photorespiration (PR) leads to significant loss of energy equivalents and previously fixed carbon in plants. Cyanobacteria possess a way to reduce the side-reaction of RuBisCO through the Carbon Concentrating Mechanism (CCM) [19]. To achieve this, RuBisCO is packaged into protein microcompartments called carboxysomes alongside the carbonic anhydrase enzyme converting HCO_3^- to CO_2, which is trapped inside the protein shell. To further increase the concentration of HCO_3^- around RuBisCO, the cell utilises the PETC's electron fluxes and ATP output to actively import CO_2 from outside the cell and transport it into the carboxysomes. Next to the central metabolism, many other sinks, such as protein and lipid production or DNA replication, require a sustained input for the cell to remain viable. In sum, the various source and sink reactions must be bal-

anced to ensure growth and viability [20].

The importance of light spectrum

Light is a critical resource for photosynthetic prokaryotes and heavily affects cell physiology [21, 22]. Significantly, beyond its intensity, the light spectrum plays a crucial role in exerting physiological control. For example, growth under various monochromatic light sources led to large differences in cyanobacterial growth rate, cell composition, and photosynthetic parameters [23]. Blue light strongly inhibits growth and can cause cell damage by disrupting the excitation balance of photosystems [24, 25, 26], resulting from the varying absorption properties of their pigments [24]. To react to changes in illumination, the cell is able to undergo both short and long-term adaptations. Over time, cells adjust the ratio of photosystems and pigment content to optimise their performance [22]. In the short term, processes like OCP-related Non-Photochemical Quenching (NPQ) [27, 28] or state transitions [29] help them adapt, though precise mechanisms of the latter are not yet fully elucidated [30]. While the scientific community agrees that the PQ redox state triggers state transitions, multiple underlying mechanisms have been proposed without a current consensus [30].

The advantage of mathematical modelling

Mathematical models integrate and condense current knowledge to identify significant parts and interactions, enabling the simulation of the effect of various external factors and internal modifications [31]. They can also provide a platform to test new hypotheses. Modifying metabolism for biotechnological purposes involves overcoming natural regulations and inhibitory mechanisms, disrupting the metabolic network's balance. However, balance is crucial for a proper photosynthetic function [20] and, thus, the viability of cyanobacteria for biotechnology. Therefore, a comprehensive understanding of metabolism is essential for effective and compatible modifications. Numerous plant models of primary metabolism helped to identify the most favourable environmental conditions, nutrient compositions, and genetic modifications to maximise the desired outputs [32]. Despite the evolutionary connection between cyanobacteria and plants, the structural differences mentioned earlier prevent the use of established plant-based models for photosynthesis. Therefore, mathematical models targeted specifically for cyanobacteria hold great promise. Established cyanobacterial models often describe broad ecosystem behaviour or specific cellular characteristics [33]. Worth mentioning here are constrained-based reconstructions of primary metabolic network [34, 26], as well as kinetic models, ranging from a simple model of non-photochemical quenching [35] to adapted plant models to study the dynamics of cyanobacteria photosynthesis [36] and models created to study proteome allocation as a function of growth rate [37]. However, non of these models provide a detailed, mechanistic description of oxygenic photosynthesis in *Synechocystis* sp. PCC 6803, including the dynamics of respiration and mechanistic description of short-term acclimation mechanisms highly sensitive to changes in light wavelengths.

With this work, we provide a detailed description of photosynthetic electron flow in cyanobacteria (as summarised in Figure 1a), parameterised to experimental data, including measurements collected under monochromatic light, in *Synechocystis* sp. PCC 6803, a unicellular freshwater cyanobacterium. Our model uses light intensity and light wavelengths as input, allowing the simulation of any combination of light sources and adaptation to the specific growth conditions. Readouts include all intermediate metabolites and carriers, most importantly ATP and NADPH, significant reaction rates, such as carbon fixation and water splitting, and the cell's PAM fluorescence. We perform Metabolic Control Analysis (MCA) [39, 40, 41] of the network in different light conditions, showing that the reactions which determine the rate of CBB flux shift from photosynthetic source reactions to sink reactions within the CBB as light intensity increases. By harnessing the power of mathematical modelling, we seek to optimise cyanobacterial production and contribute to the advancement of green biotechnology.

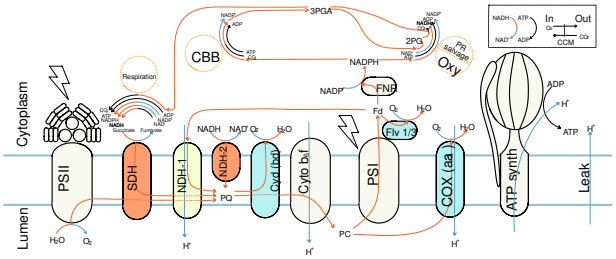

(a) Schematic overview of all reactions and compounds captured with the mathematical model.

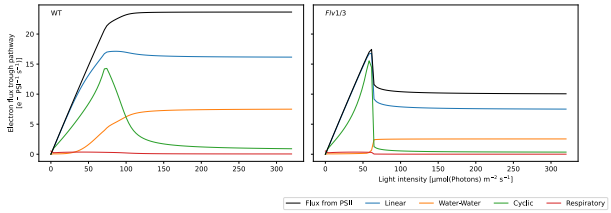

(b) Simulated steady-state fluxes through PSI associated with the possible electron pathways for increasing light intensities.

Figure 1: **Computational model of the photosynthetic and respiratory chain allowing to predict electron fluxes through alternative pathways in various strains of *Synechocystis* sp. PCC 6803.** (a) The two blue, horizontal lines indicate the thylakoid membrane. Inset ovals represent ETC proteins and complexes. The respective colouring highlights the considered components of LET (white), CET (yellow), RET (orange), and WWC (light blue). The orange circles show lumped pathways. The top-right box shows gas exchange reactions (O_2 export and active CO_2 import) and metabolic ATP and NADPH consumption. Electron and proton flows are coloured orange and blue, respectively. The PBS is shown attached to PSII. (b) Predicted electron flux through the aforementioned four electron pathways for increasing light intensities. Each value represents a steady-state flux under continuous light exposure. Simulations were run using Gaussian LED (670 nm nm, σ = 10 nm). No assumed light attenuation. Our model correctly predicts the proportion of linear electron flow (blue) to four other pathways to be around 60% [38] in wild type (WT). We predict the flux distribution for the flavodiiron (*Flv*1/3) knockout (KO) mutant. Abbreviations: 2PG: 2-phosphoglycolate, 3PGA: 3-phosphoglycerate, ADP: Adenosine diphosphate, ATP: Adenosine triphosphate, ATPsynth: ATP synthase, CBB: Calvin-Benson-Bassham cycle, CCM: Carbon Concentrating Mechanism, COX(aa_3): Cytochrome c oxidase, Cyd(bd): Cytochrome bd quinol oxidase, Cyto b_6f: Cytochrome b_6f complex, FNR: Ferredoxin-$NADP^+$ Reductase, FQ: Ferredoxin quinol reductase, Fd: Ferredoxin, Flv: Flavodiiron protein dimer 1/3, $NADP^+$: Nicotinamide adenine dinucleotide phosphate, NADPH: reduced Nicotinamide adenine dinucleotide phosphate, NAD^+: Nicotinamide adenine dinucleotide, NADH: reduced Nicotinamide adenine dinucleotide, NDH-1: NADPH dehydrogenase 1, NDH-2: NADPH dehydrogenase 2, Oxy: RuBisCO oxygenation, PC: Plastocyanine, PQ: Plastoquinone, PR: Photorespiration, PSI: Photosystem I, PSII: Photosystem II, SDH: Succinate dehydrogenase

Methods

Model description

Here, we developed a mathematical model of photosynthetic electron transport in *Synechocystis* sp. PCC 6803 (further *Synechocystis*). Our focus lay on constructing an up-to-date dynamic model of cyanobacteria photosynthesis by integrating physiological data and dynamic observations from numerous groups (pH-ranges: [42], NADPH reduction: [43], O_2 change rates: [18], CO_2 consumption: [37], PQ reduction: [44], PC, PSI, and Fd redox-states: [45], PAM-behaviour: [30], electron fluxes: [38], PAM fluorescence: [46]). Fluorescence-related parameters, including quenching and OCP constants, were fitted to PAMfluorescence curves and measurements [46]. A comprehensive list of all the model parameters utilised in this study, including values needed for unit conversion, is provided in Table S1 and Table S2 (state transition analysis separate, see below), ensuring transparency and reproducibility of our computational approach. The model has been developed in `Python` [47] using the modelling package `modelbase` [48] further exploring a highly modular approach to programming mathematical models. The model and scripts used to numerically integrate the system and to produce all figures from this manuscript are accessible at `https://gitlab.com/TPfennig/synechocystis-etc-2022`.

The model is a system of coupled Ordinary Differential Equations (ODEs) allowing us to capture the time-dependent dynamic behaviour of rates and concentrations of all described reactions and reactants (as visualised on Figure 1a and summarised in Table S3), including dynamic changes in the lumenal and cytoplasmic pH. Given the high similarity between the essential electron transport chain proteins of plants and cyanobacteria [14], the photosystems, which play a key role in capturing light energy for photosynthesis, were modelled based on the representation proposed by [49]. We included a detailed description of four possible electron circuits: Linear Electron Transport (LET), CET, RET, and WWC. We followed a reductionist approach simplifying many downstream processes into lumped reactions. The lumped CBB, PR, and metabolic consumption reactions represented the main cellular energy sinks. CBB and RuBisCO oxygenation (Oxy) were described using multiple regulatory terms, including gas and metabolite concentrations (Table S4). We also considered a simple

Carbon Concentrating Mechanism (CCM) implementation by calculating the dissolved CO_2 concentration at the cellular pH and with an actively 1000-fold increased intracellular CO_2 gas pressure. During simulations most parameters were held constant: 25 °C temperature with 230 µmol L^{-1} dissolved O_2 and 4×10^{-4} atm CO_2 in the medium. The default initial metabolite concentrations were set to literature measurements (Table S5). These "default conditions" ensured that simulations were comparable and biologically relevant. Steady-state simulations were run for 1×10^6 s. We considered that the steady-state is reached if the Euclidean norm of concentration differences between the two final time steps did not exceed 1×10^{-6} mmol mol(chl)$^{-1}$ for all concentrations aside from ATP, CO_2, and 3PGA for which the tolerance level was set to 1×10^{-4} mmol mol(chl)$^{-1}$.

Reaction kinetics

Following the principle of parsimony, all reactions where no additional regulatory mechanism was known have been implemented with first-order Mass-Action (MA) kinetics. A reaction with substrates S_i and products P_j is defined as: $\sum n_i S_i \longleftrightarrow \sum m_j P_j$ with $i, j \in \mathbb{N}$ where n_i and m_j are the stoichiometric coefficients of substrates and products, respectively. We assigned reaction directionality by calculating Gibbs free energies ($\Delta_r G'$) from the midpoint potentials of redox pairs, as done for plant photosynthesis models [49, 50]. Thus, we set reactions as irreversible except for ATP synthase, SDH, FNR, and PSII and PSI internal processes.

To simplify higher order reversible MA equations [51], we first decompose the rate equation into separate kinetic and thermodynamic components (as done for Michaelis-Menten (MM) [52]) and then simplify the kinetic part as:

$$v = \begin{cases} \text{if } \Delta_r G' < 0: & k^+ \cdot \prod c_{S_i} \cdot \left(1 - \exp(\Delta_r G'/RT)\right) \\ \text{else:} & k^- \cdot \frac{\prod c_{P_j}}{K_{eq}} \cdot \left(\exp(-\Delta_r G'/RT) - 1\right) \end{cases} \tag{1}$$

with substrate concentrations c_S, product concentrations c_P, and $K_{eq} = \prod c_{P_j}^{m_j} / \prod c_{S_i}^{n_i}$.

During the process, the equilibrium equality derived from MA, $K_{eq} = k^+/k^-$, was violated. This necessitated parameterising k^+ and k^- separately. The reactions FNR and SDH, which were deemed reversible, used rate Equation 1 with the determination of $\Delta_r G'$ during simulation.

Implementation of monochromatic and composed light sources

To consider the influence of light spectrum on photosynthetic activity, we integrated the estimation of pigment-based light absorption for PSI, PSII, and PBS [53]. This implementation enabled us to simulate various light-adapted cells by updating the parameters corresponding to measured pigment composition and photosystem ratio (e.g. in [53, 46]). Importantly, we assume that despite the wavelength-dependent energy content, all photons result in equivalent excitation of photosystems with the extra energy being lost as heat [54, 55]. We assume that PBSs can be either free, in which case the excitation is lost, or attached to a photosystem to transfer their excitation energy. The respective fractions of PBS states were fixed to literature values or measurements except for simulations of state transition mechanisms which required dynamic PBS behaviour.

Testing four possible mechanisms of state transitions

We have implemented and tested four proposed mechanisms of state transitions, based on a recent review [30]:

- **PSII-quenching Model** (default) - reduced PQ (Q_{red}) reversibly quenches PSII to $PS2_q$ with stronger excitation heat quenching
- **Spillover Model** - Q_{red} induces PSII excitation transfer to PSI
- **PBS-Mobile Model** - Q_{red} induces PBS switching from PSII to PSI
- **PBS-Detachment Model** - oxidised PQ induces detachment of PBSs from both photosystems

The mechanisms are visualised in Figure 4a. The PSII-quenching model was implemented using Hill equations and parametrised during data fitting for Figure 2a. We implemented the remaining state transitions models using simple MA kinetics (Table S6) (parameters in Table S7). We then systematically varied the parameter sets of all implementations and compared the steady-state fluorescence and PQ redox state under different lighting conditions (actinic: 440 nm at 80 µmol(photons) $m^{-2}\,s^{-1}$ or 633 nm at 50 µmol(photons) $m^{-2}\,s^{-1}$; measuring: 450 nm and 625 nm at 1 µmol(photons) $m^{-2}\,s^{-1}$).

Simulating PAM fluorescence measurements

Considering cyanobacterial optical properties of light-harvesting pigments, we estimate the fluorescence signal by calculating the weighted sum of PSI, PSII, and PBS fluorescence:

$$F = w_{PS1} \cdot F_{PS1} + w_{PS2} \cdot F_{PS2} + w_{PBS} \cdot F_{PBS} \quad (2)$$

with the weights w in `fluo_influence` (Table S1). The weights were set close to one during parameter fitting. Based on the principle of PAM measurements, the model calculates fluorescence proportional to the gain in excited internal states of PSII and PSI when adding measuring light to the growth light. Additionally, we consider fluorescence of free PBS using their light absorption [56]. The default measuring light is set to 625 nm at 1 µmol(photons) $m^{-2}\,s^{-1}$ throughout this manuscript.

Metabolic Control Analysis

Alteration of parameters like enzyme concentrations differently affects the whole system's behaviour depending on the affected reaction. Metabolic Control Analysis (MCA) measures these effects by slightly perturbing single parameters and quantifying the change in steady-state [39, 41]. The resulting control coefficients are the factor between the fractional parameter alterations and the systems' fluxes or concentrations.

We performed MCA on the model with different simulated irradiances (Figure 3a) [53]. These included the solar spectrum, a fluorescent lamp, cold and warm LEDs and Gaussian LEDs, which were approximated as Gauss curves with peaks at the respective wavelength and variance of either 10 nm (default) or 0.001 nm ("near-monochromatic") (see Figure 3a & Figure S5).

We divided the PETC components into non-overlapping sets representing the light-driven electron flow (LET + CET), respiration, RuBisCO reactions, and terminal oxidases (see appendix). The control coefficients C_{ij} of each component i's rate-determining parameter on output j were then summed up as absolutes within each set X:

$$\sum_i |C_{ij}| \text{ for } i \in X. \quad (3)$$

Results

Our analysis focuses on several key aspects: the redox state of electron carriers, carbon fixation rates in ambient air, reproduction of fluorescence dynamics under changing light conditions, simulating PAM curves, and the rates of alternative electron circuits (LET, CET, WWC) under different conditions. We used O_2 measurements [57] to check the PSII light harvesting and photochemistry implementation of the model. Our simulated steady-state O_2 rates are in qualitative agreement with the experimental data (Figure S1). The quantitative discrepancy can be due to the default set-up we have used to model the cell. Unfortunately, the exact culture conditions (e.g. density) and strain used in the reference work [57] are not known. Hence the pigment composition may differ. Additionally, we used PSII open fractions (Figure S2) to further assess the quality of our model performance.

Flux through alternative electron pathways

We simulated the steady-state flux of electrons through the PETC for four transport pathways in wild type and two *in silico* mutants exposed to a

670 nm monochromatic light (Figure 1b). We parameterised the flux through the CET to yield approximately 35 % of the total PSI electron flux [38]. As the experimental analysis [38], we found for low light intensities similar electron partitioning as in wild-type and *Flv1/3* mutants, however for higher light intensities, the predicted WWC became significant. The possible reason for such discrepancy between our results and the original work is the culture conditions (high CO_2 and pH) leading to terminal oxidase inactivity, which the model currently cannot reproduce (personal correspondence, see also [58]).

Notably, the *Flv1/3* mutant showed a faster and more substantial increase in CET with increasing light, pointing towards a balancing act of NDH-1 [45]. Interestingly, under our assumed culture conditions, the CET can only increase up to a light intensity of ca. 70 µmol(photons) $m^{-2}\,s^{-1}$ after which the LET stagnates and the WWC increases strongly. Flv mutants experienced this collapse at lower light intensities. Apparently, this critical light intensity marks a change in *Synechocystis* photosynthetic metabolism. In addition to simulating electron flow, our model can be used to probe the redox state of the cell, pH, and additional fluxes through key biochemical reactions (Figure S3). This allows us to investigate the effect of imposed mutations on the PETC.

Photosynthesis dynamics captured via fluorescence measurements

Using experimental measurements [46] (pigment concentrations, photosystems ratios, and expected PBS-attachment - method currently under review), we adapted the model to represent a *Synechocystis* strain grown under 435 nm monochromatic light and performed a PAM experiment *in silico*. By monitoring cell responses to changing light conditions, we captured light responses via state transitions and non-photochemical quenching and relaxation. Simulations were run using the same light protocol of blue and red light, as used *in vivo* [46], and parameters controlling the fluorescence composition, state transitions, NPQ, and CET were updated to get the best agreement between our simulated trace and the original data (Figure 2a). Because of measuring proto-

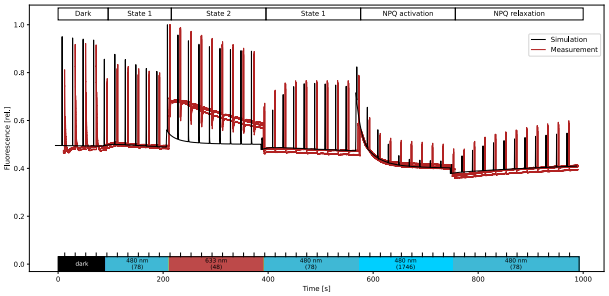

(a) Simulated (red) and measured (black) fluorescence dynamics of a single cell using the PAM technique.

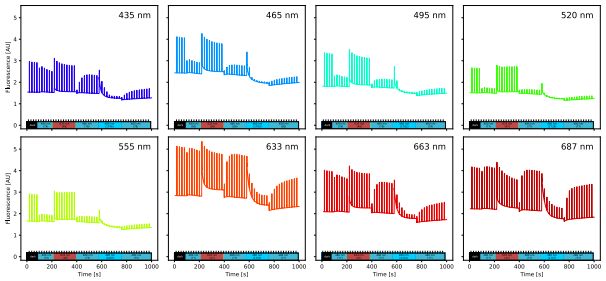

(b) Simulated PAM fluorescence traces with strains adapted to different monochromatic lights.

Figure 2: **Pulse Amplitude Modulation (PAM) chlorophyll fluorescence signal *in vivo* and *in silico*.** The fluorescence signal has been calculated using (Equation 2). (a) The simulated light protocol mirrored the experimental setup with a cell grown under 435 nm light [46], where we used several different light wavelengths and intensities to trigger a response from respective photosynthetic electron transport chain components. By monitoring cell responses to these light conditions, we captured light responses via state transitions and non-photochemical quenching and relaxation (as described in the upper bar). The simulated fluorescence in state 2 is underestimated, likely due to the assumed Quasi-Steady-State of the PSII. Furthermore, the underestimated Peak Fluorescence during NPQ activation likely stems from slow CBB activation and resulting PSII quenching. The lower bar depicts the light intensity (considering light attenuation) and wavelength (in parentheses, in µmol(photons) $m^{-2}\,s^{-1}$) (lights used: 480 nm at 80 µmol(photons) $m^{-2}\,s^{-1}$ and 1800 µmol(photons) $m^{-2}\,s^{-1}$ and 633 nm at 50 µmol(photons) $m^{-2}\,s^{-1}$, saturating pulse: respective wavelength at 2600 µmol(photons) $m^{-2}\,s^{-1}$). See the supplemental information for the fitted parameter values. (b) Simulated PAM fluorescence signal with the same light protocol as described in (a) for cells grown under different monochromatic lights (435 nm for reference). The simulations were adapted to the given strain by changing the parameters corresponding to pigment composition. The parameters which were fit in (a) were reused in (b).

col discrepancies, we also lowered the simulated pulse light intensity. We found that increasing the CET rate twofold provided better recovery of the fluorescence signal and CET rates closer to experimentally measured values [38]. This suggests that cells grown under PSI-preferred light might adapt CET to respond to the PSI-preferred illumination. Our simulation predicted especially well the transition to state 1 in blue light and the NPQ action and relaxation. Interestingly, a high Dark Peak Fluorescence (F_m) was found, implying the cells did not fully transition to state 2 in darkness [30]. A strong, non-linear dependency of our PSII QSS function on reduced PQ likely caused the deviance in the state 2 Steady-State Fluorescence (F) level. Furthermore, the underestimation of peak fluorescence during OCP activation might be due to our assumed slow CBB activation, causing PSII quenching. The model correctly predicted the 480 nm saturation pulses to be non-saturating and induce fluorescence quenching, as confirmed by follow-up experiments ([46], see their Fig. S14; also here Figure S4). To further explore the predictive power of this model we further simulated fluorescence signal for cells grown under monochromatic light, exposed to the same light protocol (Figure 2b). The adapted cells showed the strong effects of altered pigment compositions on cellular reactions and fluorescence.

Common light sources affect the metabolic control differently

Photosynthesis experiments can be conducted with many different light sources that are equivalent in photon output but differ in the spectrum. To further investigate how these spectral differences affect cellular metabolism, we simulated the model with different near-monochromatic and "white" light sources: solar irradiance, fluorescence lamp, and cool and warm white LED (Figure 3a). For each light, we simulated the model to steady-state to perform MCA (Figure 3b). We slightly perturbed single parameters of the PETC components and quantified the effect on the steady-state fluxes and concentrations. A high control coefficient represents a strong dependency of the pathway flux on changes to that parameter, with control in a metabolic network usually being distributed across multiple reactions. A single parameter being in full control of the flux through a network would represent the case of a typical bottleneck, but this rarely occurs in biological systems [39, 41]. We show that the electron pathway-specific control differs between the simulated light sources. The model suggests that, at lower intensities of blue-centric spectra (solar and cool white LED), the control mainly lies within light-driven (linear and cyclic) electron flow (Figure 3b). Red-centric spectra (fluo-

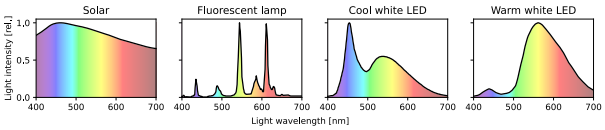

(a) Analysed, common light sources

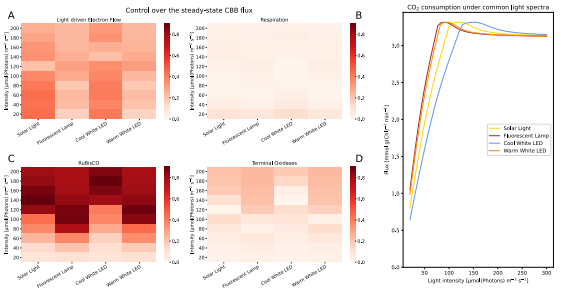

(b) Flux Control Coefficients calculated for four key biochemical reactions.

(c) Steady State Flux through CBB under the different light sources and intensities

Figure 3: **Systematic analysis of a single-cell performance under various light sources.** (a) The light spectra of four light sources, including often used in the lab "white" light LED panels. (b) Results of Metabolic Control Analysis (MCA) performed for the four light sources. We simulated the model under the lights in (a) with a range of intensities from 20 µmol(photons) m^{-2} s^{-1} to 200 µmol(photons) m^{-2} s^{-1} to steady-state. Small perturbations in the components' rate parameters were tested to quantify their effect on the target fluxes/concentrations. We then summed up the absolute control coefficients within selected pathways (Equation 3). Higher values signify stronger pathway control. The model shows that the distinct light spectra result in a differential distribution of control over the system. Especially, the impact of CET and the CBB varies. (c) Steady-state Flux through CBB under the lights in (a), simulated over different light intensities. No assumed light attenuation.

rescent lamp and warm white LED) seem to induce less light-driven control under the same conditions (Figure 3c). That means the photosynthetic production of NADPH and ATP is less dependent on any one component, and the maximum is reached at lower light intensities. For increasing light, the CBB gains system control in all tested spectra, marking a point of induced sink limitation.

Repeating the analysis with simulated monochromatic lights, we found similar differences between preferentially chlorophyll ("blue-centric") or PBS ("red-centric") absorbed light (Figure S5). The earliest switch to sink limitation was found in 624 nm light, while weakly absorbed light (such as 480 nm) seems to have little control effect. Using the model, the control of single components, such as photosystems, can also be investigated (Figure S6).

Model as a platform to test alternative mechanisms of state transition

We defined four functions representing the mechanism of state transitions with the PSII-quenching model [59] as the default (Figure 4b). Therein, a more reduced PQ pool causes a higher fraction of PSII excitations to be lost as heat. Additionally, the Spillover Model, where state 2 induces PSII excitation energy transfer to PSI; the PBS-Mobile model, where PBS attach preferentially to PSI or PSII in states 1 and 2, respectively; and the PBS-detachment Model, where PBS detach from the photosystems in state 1 were tested [59, 30]. We then performed a typical PAM simulation under each assumption and investigated the overall fluorescence kinetics (Figure 4c). Noticeably, the PBS-detachment Model predicted an unexpectedly high Dark Steady-State Fluorescence (F_0) due to the only partially reduced PQ pool. We additionally calculated the relative difference of PQ reduction under state 2 lighting to a model with no state transitions, and the reduction of Peak Fluorescence (F'_m) from state 1 to state 2 (Figure 4c). Here, the PBS-detachment implementation model showed little potential to alleviate steady-state PQ reduction in state 2 (Figure 4c). This balancing effect, however, has been experimentally observed and is seen as the main objective for state transitions [30]. The remaining state transition models showed comparable balancing potentials. Furthermore, within the parameter-varied simulations, the spillover and PBS-detachment models showed less reduction of the F'_m-level during state 2. Therefore, these models seem less capable of reproducing experimental fluorescence traces where this reduction is often more than 10 % (Figure 2a, [18], [30]). PBS-involving models also produced strongly differing fluorescence traces when simulated with 450 nm measuring light outside of the PBS absorption spectrum (Figure S7). Comparing experimental fluorescence with different measuring lights might, therefore, be viable for testing PBS-involvement in state transitions.

Model as a platform to test optimal light for biotechnological exploration

To showcase the biotechnological usability of this work, we analysed the *Synechocystis* productivity for various light sources. Simulations of CO_2 consumption (Figure 5) agree with the previous control analysis (Figure S5). The highest flux is reached at or below 100 µmol(photons) $m^{-2}\,s^{-1}$ for most wavelengths, whereby 40 µmol(photons) $m^{-2}\,s^{-1}$ of 624 nm light are already sufficient. Therefore, red light seems to be most efficient for the production of sugars, either for the production of biomass or secretion of e.g. sucrose.

Cyanobacteria show potential as cell factories for the production of terpenoids from CO_2 or as whole-cell biocatalysts, which require different ratios of NADPH, ATP and carbon. To identify the optimal light conditions for these exemplary processes, additional energy and carbon sink reactions were added to the model, and production was simulated with different light conditions (Figure 5). For terpenoid production from CO_2, optimal lighting conditions are largely the same as for the CBB. Thus, carbon fixation appears to be a more significant controlling factor than the energy cost of their production. The production of sucrose and glycogen with a higher ATP:NADPH ratio shows locally enhanced production in the chlorophyll absorption spectrum (e.g., 440 nm and 100 µmol(photons) $m^{-2}\,s^{-1}$), which

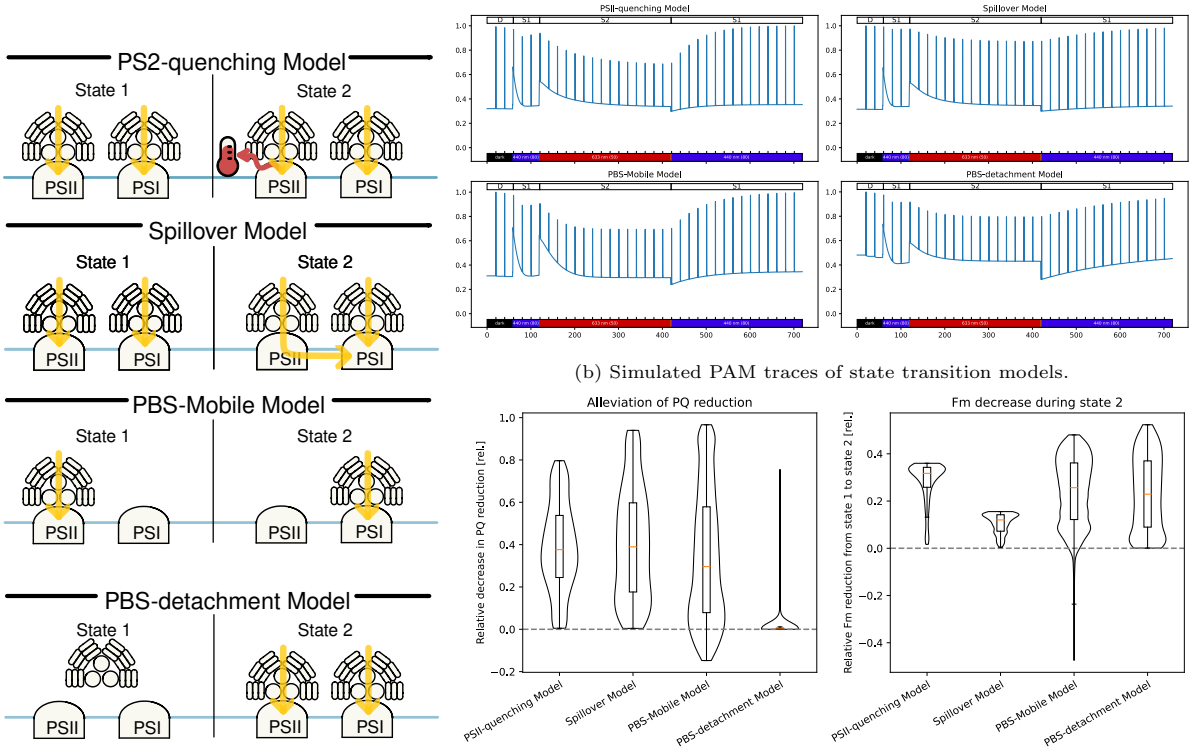

(a) Schematic representation of four state transition models, after a recent review [30].

(b) Simulated PAM traces of state transition models.

(c) Simulated alleviation of PQ reduction and fluorescence difference.

Figure 4: **Testing possible mechanisms of state transitions.** (a) Four possible mechanisms of state transitions have been implemented and tested with the model. The PSII-quenching model is the default. The alternative implementations are exemplary and based on a recent review [30]. (b) Comparison of simulated fluorescence curves. The fluorescence signal has been calculated using (Equation 2). The simulated light protocol mirrored a state transition experiment where low-light illuminations were used to trigger states 1 and 2. The alternative implementations can reproduce fluorescence traces similar to the PSII-quenching model. The PBS-detachment model, however, predicts an elevated Dark Steady-State Fluorescence (F_0). (c) Left) The relative difference of PQ reduction under state 2 lighting to a model with no state transitions. The respective implementations' parameters were systematically varied, and the distribution of relative reduction-alleviation is shown as violin plots with quantiles as boxplots. Right) The reduction of Dark Peak Fluorescence (F_m) from state 1 to state 2 in the model variations. The distribution is also shown as violin plots with inset boxplots. The spillover implementation shows a much smaller difference in F_m between the states. The lower bar in (b) depicts the light intensity (considering light attenuation) and wavelength (in parentheses, in µmol(photons) $m^{-2}\,s^{-1}$). The upper bar shows the induced state (lights used: 440 nm at 80 µmol(photons) $m^{-2}\,s^{-1}$ and 633 nm at 50 µmol(photons) $m^{-2}\,s^{-1}$, saturating pulse: 15 000 µmol(photons) $m^{-2}\,s^{-1}$ of the respective wavelength). No assumed light attenuation.

is more pronounced for further increased ATP demand (see Glycogen + ATP in Figure 5c, representing high glycogen turnover). Overall, we see strong light preferences for the production of ATP (stimulation of PSI and CET without activation of the water-water cycle) and NADPH (624 nm light) (Figure 5c), which seem to determine the light preference of a target reaction. While these results were obtained for an unadapted cell, our model allows to repeat such analyses with any adapted pigment composition (Figure S8).

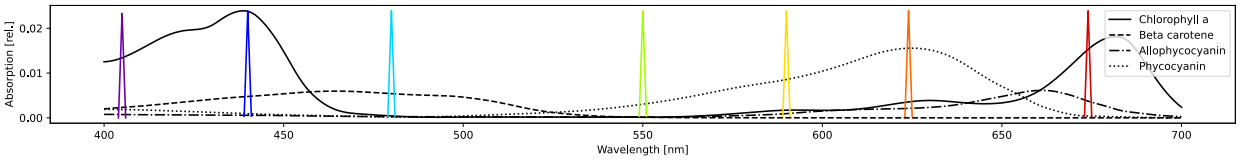

(a) Monochromatic light and pigment absorption spectra.

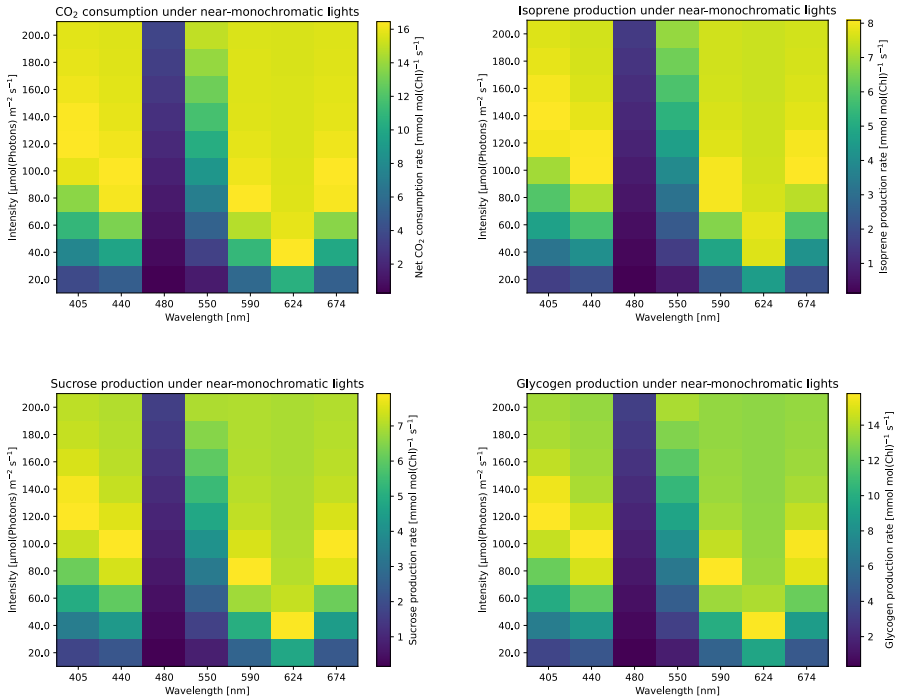

(b) Simulated CO_2 fixation and production rates of biotechnological relevant sinks.

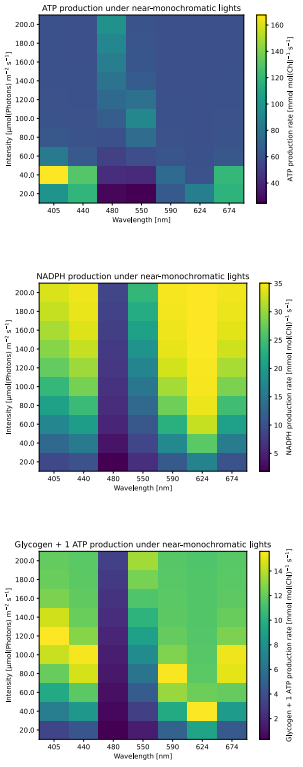

(c) Simulated production rates of ATP, NADPH, and glycogen with theoretically increased high ATP demand.

Figure 5: **Simulated steady-state rates of CO_2 fixation or production of target compounds under monochromatic lights with varying intensities.** (a) Illumination with monochromatic Gaussian LEDs. The lights are shown as coloured spikes in the top panel, together with the relative absorption spectra of selected pigments. (b) The model was simulated to steady-state under illumination with different near-monochromatic lights within the visible range. Different target sinks were added in each simulation to measure the maximum possible production rate. Shown are the CO_2consumption, a sink with isoprene synthesis-like stoichiometry representing terpenes (3 ATP, 1 NADPH, 4 Fd_{red} $\approx$ 2 NADPH, 2 3PGA), sucrose production (3 ATP, 2 NADPH, 2 3PGA), and glycogen production (2 ATP, 1 NADPH, 1 3PGA). (c) Additional steady-state production analysis of pure ATP, NADPH and a theoretical glycogen sink with increased ATP consumption (3 ATP, 1 NADPH, 1 3PGA) representing a scenario with high glycogen turnover. The CO_2 fixation rate reaches a maximum under most wavelengths, except for 480 nm and 550 nm. For 624 nm, the maximal rate is reached at the lowest light intensity. Depending on the ATP and NADPH consumption, the light preference of sink reactions differs distinctly. No assumed light attenuation.

Discussion

In this work, we present our mathematical ODE-based photosynthesis model as a quantitative *in silico* tool with high predictive power and customisability. The model contains all major steps of *Synechocystis* photosynthetic electron flow, from light capture to CO_2 fixation [15] and a description of the respiratory chain embedded within the same membrane. Furthermore, cyanobacteria-specific mechanisms were implemented in the model, including state transitions and OCP-mediated NPQ [27, 60, 30]. In contrast to other existing dynamic models of photosynthesis, our model can simulate illumination within the full visible spectrum (400 nm to 700 nm), also accounting for the pigment composition of the strain. Results obtained with our model provide insights into the intricate dynamics of the photosynthetic process under various light conditions. Our analyses focus on several key aspects of photosynthetic dynamics: Flux through alternative electron pathways, the redox state of electron carriers, carbon fixation rates in ambient air, and prediction of fluorescence dynamics under changing light conditions modulating PAM experiments.

The model was validated against published measurements of gas exchange rates and electron pathway fluxes (Figure S1). The good estimation of oxygen production rates supports our pigment-specific implementation of light absorption, which allows for a better assessment of the possible effect of photosystem imbalance [24, 53]. The model also satisfactorily estimates flux through the four electron transport pathways. Our simulations show the dominance of LET (ca. 60 %; [38]), which is supplemented by CET in low light and WWC in high light (Figure 1 b). Moreover, the model can be used to gain in-depth information on the system's behaviour using *in-silico* mutants. Simulations of a *Flv* knockout (KO) mutant showed a redox alleviating effect of CET under high light (Figure 1 b). A link between the involved proteins' functions, Flv and NDH-1, has been reported previously [61].

Our model has been used as a platform to test alternative mechanisms of state transitions for which there is no literature consensus [30] on the basis of PQ reduction and PAM fluorescence. Our simulations support a PSII quenching model [59] rather than PBS detachment and spill-over, as suggested previously [30]. We also found that the involvement of PBS might be testable when comparing different measuring lights.

The model can further estimate the system's steady-state control distribution through MCA to investigate the effect of different light source spectra. We found differential productivity control under simulated solar illumination, a fluorescent lamp, and cold and warm white LEDs (Figure 3). Light preferentially exciting PSI showed pronounced source-control, meaning that changes to the photosynthetic production pathways of NADPH and ATP influenced productivity more and stronger light was needed. At higher light intensities, the strategy promising better productivity would involve increasing carbon fixation by e.g. additionally increasing the CO_2 concentration around RuBisCO [62], engineering RuBisCO itself [63] or introducing additional carbon sinks such as sucrose, lactate, terpenoids or 2,3-butanediol [64, 65, 66, 67]. With the implementation of the spectral resolution, our model could also simulate cellular behaviour in high cell densities (e.g. bioreactors), where the light conditions might differ throughout the culture [68]. We show that lighting in the orange-red spectrum requires the lowest intensity to saturate the photosystems, with a warm-white LED showing the same efficiency as a fluorescent light bulb, an important consideration when calculating process costs (Figure 3c). Additionally, we investigated the effect of different monochromatic lights on the production of biotechnologically relevant products: Sugars, terpenoids, ATP or NADPH (Figure 5). We found that for the selected conditions, the optimal light for high CO_2fixation and terpenoid production were similar, although their ATP and NADPH requirements are different. A recent study also found 405 nm illumination to increase isoprene and xanthophyll production and alter carbon allocation, which our model does not reproduce, possibly due to downstream processes [26]. Simulated reactions with higher ATP:NADPH ratio, like sucrose or glycogen synthesis, showed a mixed light preference of NADPH (624 nm) and ATP (exciting PSI at

intensities not triggering the WWC; ca. 440 nm or 680 nm $< 100\,\mu\text{mol(photons)}\,\text{m}^{-2}\,\text{s}^{-1}$). These results again support the need to test and optimise light conditions for each application on its own, as the stoichiometry of the desired process changes light requirements. Recently, two-phase processes have been used to increase titers in cyanobacterial biotechnology, arresting growth to direct all carbon towards a product [69]. Our model suggests that as a part of this process, changes in light colour could be used to intentionally create imbalances in metabolism and direct flux to the desired product according to the energetic needs of the particular pathway.

For each simulation, we assume fixed pigment composition and light absorption capacity, thus, analysing a given cell state. We, therefore, cannot predict long-term cellular adaption to different environmental conditions, but adaptations of the cell to light, growth phases and the stress responses resulting from e.g. high light intensities can be used as new inputs according to experimental data. Furthermore, our model considers the CBB as the main sink for energy equivalents which might not be the case for cells with higher growth rates, where the production of other biomass components can become more significant (e.g. glycogen [70]). Additionally, further improvements of the currently significantly simplified CCM and photorespiratory salvage functions could be beneficial, also due to the engineering efforts in building pyrenoid-based CO_2-concentrating mechanisms *in-planta* [71].

Our model follows the dynamic change in the lumenal and cytoplasmic pH but is lacking the full description of *pmf*. An envisaged step of further development will be the integration of the membrane potential $\Delta\Psi$ into the model and simulation of ion movement, as presented in several mathematical models for plants [72, 73]. It would be moreover interesting to include the spatial component into the model, accounting for the dynamics of thylakoid membranes, as revealed by [74]. Thanks to our computational implementation of the model using the package `modelbase` [48], the model is highly modular, and the addition of new pathways or the integration of other published models (e.g. a recent CBB model [75]) should not constitute a technical challenge.

In conclusion, the presented computational model serves as a valuable tool for investigating cyanobacteria-specific photosynthetic electron flow. By successfully reproducing experimental data, including state-of-the-art fluorescence measurements, we gained insights into the unique behaviour of cyanobacteria under monochromatic and composed light. Notably, our findings suggest that PSII-internal quenching is a probable state transition mechanism, providing theoretical evidence for a yet unclear photoprotective mechanism. We are confident that by shedding light on cyanobacterial photosynthetic behaviour, this model will greatly contribute to future research in synthetic biology, microbial engineering, and the advancement of photo-biotransformation using cyanobacteria.

Acknowledgements

We would like to thank Ilka Axmann and Marion Eisenhut for the initial conversations on the physiology of cyanobacteria that motivated construction of this detailed model, and David Fuente for discussion on the cyanobacterial absorption and pigment compositions.

Funding statement

This work was funded by the Deutsche Forschungsgemeinschaft under Germany´s Excellence Strategy – EXC-2048/1 – project ID 390686111 (TP, OE, AM); Deutsche Forschungsgemeinschaft Research Grant - project ID 420069095 (EK, AN, AM); Ministry of Education, Youth and Sports of CR within the CzeCOS program (grant number LM2018123), under the OP RDE (grant number CZ.02.1.01/0.0/0.0/16 026/0008413 'Strategic Partnership for Environmental Technologies and Energy Production') (TZ, JC); as well as by the National Research, Development and Innovation Office of Hungary, NKFIH (awards K 140351 and RRF-2.3.1-21-2022-00014 (GB).

Authors contribution

EK, AM initiated the project; TP, EK developed the model; EK, TP, and AN performed simulations; TZ

conducted additional measurements; TP, EK, AE, and AM wrote the manuscript; all authors discussed, read, and approved the manuscript.

References

[1] Malihe Mehdizadeh Allaf and Hassan Peerhossaini. Cyanobacteria: Model Microorganisms and Beyond, 4 2022.

[2] Sophie De Vries and Jan De Vries. Evolutionary genomic insights into cyanobacterial symbioses in plants, 8 2022.

[3] Jay Kumar, Divya Singh, Madhu B. Tyagi, and Ashok Kumar. Cyanobacteria: Applications in Biotechnology. In *Cyanobacteria*, chapter 16, pages 327–346. Elsevier, 12 2019.

[4] K Benedikt Möllers, David Cannella, Henning Jørgensen, and Niels-Ulrik Frigaard. Cyanobacterial biomass as carbohydrate and nutrient feedstock for bioethanol production by yeast fermentation. *Biotechnology for Biofuels*, 7(1):64, 12 2014.

[5] Stephanie G. Hays and Daniel C. Ducat. Engineering cyanobacteria as photosynthetic feedstock factories. *Photosynthesis Research*, 123(3):285–295, 3 2015.

[6] Mrinal Kumar Sarma, Sharbani Kaushik, and Pranab Goswami. Cyanobacteria: A metabolic power house for harvesting solar energy to produce bio-electricity and biofuels. *Biomass and Bioenergy*, 90:187–201, 7 2016.

[7] Ewa Żymańczyk-Duda, Sunday Ocholi Samson, Małgorzata Brzezińska-Rodak, and Magdalena Klimek-Ochab. Versatile Applications of Cyanobacteria in Biotechnology. *Microorganisms*, 10(12), 12 2022.

[8] Oliver Klaus, Fabienne Hilgers, Andreas Nakielski, Dennis Hasenklever, Karl Erich Jaeger, Ilka M. Axmann, and Thomas Drepper. Engineering phototrophic bacteria for the production of terpenoids. *Current Opinion in Biotechnology*, 77:102764, 10 2022.

[9] Jens Appel, Vanessa Hueren, Marko Boehm, and Kirstin Gutekunst. Cyanobacterial in vivo solar hydrogen production using a photosystem I–hydrogenase (PsaD-HoxYH) fusion complex. *Nature Energy*, 5(6):458–467, 6 2020.

[10] David J Lea-Smith, Paolo Bombelli, Ravendran Vasudevan, and Christopher J Howe. Photosynthetic, respiratory and extracellular electron transport pathways in cyanobacteria. *Biochimica et Biophysica Acta (BBA) - Bioenergetics*, 1857(3):247–255, 3 2016.

[11] Christine M. Lewis, Justin D. Flory, Thomas A. Moore, Ana L. Moore, Bruce E. Rittmann, Wim F.J. Vermaas, César I. Torres, and Petra Fromme. Electrochemically Driven Photosynthetic Electron Transport in Cyanobacteria Lacking Photosystem II. *Journal of the American Chemical Society*, 144(7):2933–2942, 2 2022.

[12] Gwenaëlle Moal and Bernard Lagoutte. Photoinduced electron transfer from photosystem I to NADP+: Characterization and tentative simulation of the in vivo environment. *Biochimica et Biophysica Acta (BBA) - Bioenergetics*, 1817(9):1635–1645, 9 2012.

[13] Allison M.L. van de Meene, Martin F. Hohmann-Marriott, Wim F.J. Vermaas, and Robert W. Roberson. The three-dimensional structure of the cyanobacterium Synechocystis sp. PCC 6803. *Archives of Microbiology*, 184(5):259–270, 1 2006.

[14] Jinlan Gao, Hao Wang, Qipeng Yuan, and Yue Feng. Structure and Function of the Photosystem Supercomplexes. *Frontiers in Plant Science*, 9:357, 3 2018.

[15] David J. Lea-Smith and Guy T. Hanke. Electron Transport in Cyanobacteria and Its Potential in Bioproduction. In *Cyanobacteria Biotechnology*, pages 33–63. Wiley, 5 2021.

[16] Ulrich Schreiber. Pulse-Amplitude-Modulation (PAM) Fluorometry and Saturation Pulse Method: An Overview. In *Chlorophyll a Fluorescence*, number January 2004, pages 279–319. Springer Netherlands, Dordrecht, 2004.

[17] Douglas Campbell, Vaughan Hurry, Adrian K. Clarke, Petter Gustafsson, and Gunnar Öquist. Chlorophyll Fluorescence Analysis of Cyanobacterial Photosynthesis and Acclimation. *Microbiology and Molecular Biology Reviews*, 62(3):667–683, 9 1998.

[18] R. Milou Schuurmans, Pascal van Alphen, J. Merijn Schuurmans, Hans C. P. Matthijs, and Klaas J. Hellingwerf. Comparison of the Photosynthetic Yield of Cyanobacteria and Green Algae: Different Methods Give Different Answers. *PLOS ONE*, 10(9):e0139061, 9 2015.

[19] Robert L. Burnap, Martin Hagemann, and Aaron Kaplan. Regulation of CO2concentrating mechanism in cyanobacteria, 1 2015.

[20] David M. Kramer and John R. Evans. The importance of energy balance in improving photosynthetic productivity. *Plant Physiology*, 155(1):70–78, 2011.

[21] Björn Andersson, Chen Shen, Michael Cantrell, David S. Dandy, and Graham Peers. The fluctuating cell-specific light environment and its effects on cyanobacterial physiology. *Plant Physiology*, 181(2):547–564, 2019.

[22] Marcel Dann, Edgardo M. Ortiz, Moritz Thomas, Arthur Guljamow, Martin Lehmann, Hanno Schaefer, and Dario Leister. Enhancing photosynthesis at high light levels by adaptive laboratory evolution. *Nature Plants*, 7(5):681–695, 5 2021.

[23] Gábor Bernát, Tomáš Zavřel, Eva Kotabová, László Kovács, Gábor Steinbach, Lajos Vörös, Ondřej Prášil, Boglárka Somogyi, and Viktor R Tóth. Photomorphogenesis in the Picocyanobacterium Cyanobium gracile Includes Increased Phycobilisome Abundance Under Blue Light, Phycobilisome Decoupling Under Near Far-Red Light, and Wavelength-Specific Photoprotective Strategies. *Frontiers in Plant Science*, 12:352, 3 2021.

[24] Veerle M. Luimstra, J. Merijn Schuurmans, Carolina F. M. de Carvalho, Hans C. P. Matthijs, Klaas J. Hellingwerf, and Jef Huisman. Exploring the low photosynthetic efficiency of cyanobacteria in blue light using a mutant lacking phycobilisomes. *Photosynthesis Research*, 141(3):291–301, 9 2019.

[25] Veerle M Luimstra, J Merijn Schuurmans, Antonie M Verschoor, Klaas J Hellingwerf, Jef Huisman, and Hans C P Matthijs. Blue light reduces photosynthetic efficiency of cyanobacteria through an imbalance between photosystems I and II. *Photosynthesis Research*, 138(2):177–189, 11 2018.

[26] João S. Rodrigues, László Kovács, Martin Lukeš, Rune Höper, Ralf Steuer, Jan Červený, Pia Lindberg, and Tomáš Zavřel. Characterizing isoprene production in cyanobacteria – Insights into the effects of light, temperature, and isoprene on Synechocystis sp. PCC 6803. *Bioresource Technology*, 380:129068, 7 2023.

[27] Diana Kirilovsky and Cheryl A. Kerfeld. The Orange Carotenoid Protein: a blue-green light photoactive protein. *Photochemical & Photobiological Sciences*, 12(7):1135–1143, 7 2013.

[28] Cheryl A. Kerfeld, Matthew R. Melnicki, Markus Sutter, and Maria Agustina Dominguez-Martin. Structure, function and evolution of the cyanobacterial orange carotenoid protein and its homologs. *New Phytologist*, 215(3):937–951, 8 2017.

[29] Diana Kirilovsky, Radek Kaňa, and Ondřej Prášil. Mechanisms Modulating Energy Arriving at Reaction Centers in Cyanobacteria. In Barbara Demmig-Adams, Gyozo Garab, William Adams III, and Govindjee, editors, *Non-Photochemical Quenching and Energy*

Dissipation in Plants, Algae and Cyanobacteria, pages 471–501. Springer Netherlands, Dordrecht, 2014.

[30] Pablo I Calzadilla and Diana Kirilovsky. Revisiting cyanobacterial state transitions. *Photochemical & Photobiological Sciences*, 19(5):585–603, 5 2020.

[31] Andreas Karoly Gombert and Jens Nielsen. Mathematical modelling of metabolism. *Current Opinion in Biotechnology*, 11(2):180–186, 4 2000.

[32] Thierry Fourcaud, Xiaopeng Zhang, Alexia Stokes, Hans Lambers, and Christian Körner. Plant growth modelling and applications: The increasing importance of plant architecture in growth models, 5 2008.

[33] Stefanie Westermark and Ralf Steuer. Toward Multiscale Models of Cyanobacterial Growth: A Modular Approach. *Frontiers in Bioengineering and Biotechnology*, 4:95, 12 2016.

[34] Henning Knoop, Yvonne Zilliges, Wolfgang Lockau, and Ralf Steuer. The Metabolic Network of Synechocystis sp. PCC 6803: Systemic Properties of Autotrophic Growth. *Plant Physiology*, 154(1):410–422, 9 2010.

[35] Maxim Y Gorbunov, Fedor I Kuzminov, Victor V Fadeev, John Dongun Kim, and Paul G Falkowski. A kinetic model of non-photochemical quenching in cyanobacteria. *Biochimica et Biophysica Acta - Bioenergetics*, 1807(12):1591–1599, 2011.

[36] A V Vershubskii, V I Mishanin, and A N Tikhonov. Modeling of the photosynthetic electron transport regulation in cyanobacteria. *Biochemistry (Moscow) Supplement Series A: Membrane and Cell Biology*, 31(2):110–128, 7 2014.

[37] Tomáš Zavřel, Marjan Faizi, Cristina Loureiro, Gereon Poschmann, Kai Stühler, Maria Sinetova, Anna Zorina, Ralf Steuer, and Jan Červený. Quantitative insights into the cyanobacterial cell economy. *eLife*, 8, feb 2019.

[38] Marius L. Theune, Sarah Hildebrandt, Anja Steffen-Heins, Wolfgang Bilger, Kirstin Gutekunst, and Jens Appel. In-vivo quantification of electron flow through photosystem I – Cyclic electron transport makes up about 35% in a cyanobacterium. *Biochimica et Biophysica Acta - Bioenergetics*, 1862(3):148353, 2021.

[39] R. Heinrich, S.M. Rapoport, and T.A. Rapoport. Metabolic regulation and mathematical models. *Progress in Biophysics and Molecular Biology*, 32(C):1–82, 1978.

[40] Jan-Hendrik S Hofmeyr. Metabolic control analysis in a nutshell. *Proceedings of the 2nd International Conference on Systems Biology*, (ii):291–300, 2001.

[41] Rafael Moreno-Sánchez, Emma Saavedra, Sara Rodríguez-Enríquez, and Viridiana Olín-Sandoval. Metabolic Control Analysis: A tool for designing strategies to manipulate metabolic pathways. *Journal of Biomedicine and Biotechnology*, 2008(1), 2008.

[42] Shimshon Belkin, Rolf J. Mehlhorn, and Lester Packer. Proton Gradients in Intact Cyanobacteria. *Plant Physiology*, 84(1):25–30, may 1987.

[43] Jason W. Cooley and Wim F. J. Vermaas. Succinate Dehydrogenase and Other Respiratory Pathways in Thylakoid Membranes of Synechocystis sp. Strain PCC 6803: Capacity Comparisons and Physiological Function. *Journal of Bacteriology*, 183(14):4251–4258, jul 2001.

[44] Sergey Khorobrykh, Tatsuhiro Tsurumaki, Kan Tanaka, Taina Tyystjärvi, and Esa Tyystjärvi. Measurement of the redox state of the plastoquinone pool in cyanobacteria. *FEBS Letters*, 594(2):367–375, jan 2020.

[45] Lauri Nikkanen, Anita Santana Sánchez, Maria Ermakova, Matthias Rögner, Laurent Cournac,

and Yagut Allahverdiyeva. Functional redundancy between flavodiiron proteins and NDH-1 in Synechocystis sp. PCC 6803. *The Plant Journal*, 103(4):1460–1476, aug 2020.

[46] Tomáš Zavřel, Anna Segečová, László Kovács, Martin Lukeš, Zoltán Novák, Milán Szabó, Boglárka Somogyi, Ondřej Prášil, Jan Červený, and Gábor Bernát. Photo-physiological Acclimation in Synechocystis sp. PCC 6803 Provides Insight into Growth Limitation in Underwater Spectra. *bioRxiv*, 2023.

[47] Guido Van Rossum and Fred L Drake. *Python 3 Reference Manual*. CreateSpace, Scotts Valley, CA, 2009.

[48] Marvin van Aalst, Oliver Ebenhöh, and Anna Matuszyńska. Constructing and analysing dynamic models with modelbase v1.2.3: a software update. *BMC Bioinformatics*, 22(1):203, 12 2021.

[49] Oliver Ebenhöh, Geoffrey Fucile, Giovanni Finazzi, Jean David Rochaix, and Michel Goldschmidt-Clermont. Short-term acclimation of the photosynthetic electron transfer chain to changing light: A mathematical model. *Philosophical Transactions of the Royal Society B: Biological Sciences*, 369(1640):20130223, apr 2014.

[50] Anna Matuszyńska, Nima P. Saadat, and Oliver Ebenhöh. Balancing energy supply during photosynthesis – a theoretical perspective. *Physiologia Plantarum*, 166(1):392–402, may 2019.

[51] Wolfram Liebermeister, Jannis Uhlendorf, and Edda Klipp. Modular rate laws for enzymatic reactions: thermodynamics, elasticities and implementation. *Bioinformatics*, 26(12):1528–1534, 6 2010.

[52] Elad Noor, Avi Flamholz, Wolfram Liebermeister, Arren Bar-Even, and Ron Milo. A note on the kinetics of enzyme action: A decomposition that highlights thermodynamic effects. *FEBS Letters*, 587(17):2772–2777, 9 2013.

[53] David Fuente, Dusan Lazar, Jose Vicente Oliver-Villanueva, and Javier F. Urchueguía. Reconstruction of the absorption spectrum of Synechocystis sp. PCC 6803 optical mutants from the in vivo signature of individual pigments. *Photosynthesis Research*, 147(1):75–90, jan 2021.

[54] Jeremy Harbinson and Eva Rosenqvist. An Introduction to Chlorophyll Fluorescence. In *Practical Applications of Chlorophyll Fluorescence in Plant Biology*, pages 1–29. Springer US, Boston, MA, 2003.

[55] Dušan Lazár. A word or two about chlorophyll fluorescence and its relation to photosynthesis research; a text for Ph.D. students, 5 2016.

[56] Alonso M. Acuña, Joris J. Snellenburg, Michal Gwizdala, Diana Kirilovsky, Rienk van Grondelle, and Ivo H. M. van Stokkum. Resolving the contribution of the uncoupled phycobilisomes to cyanobacterial pulse-amplitude modulated (PAM) fluorometry signals. *Photosynthesis Research*, 127(1):91–102, 1 2016.

[57] R. Milou Schuurmans, J. Merijn Schuurmans, Martijn Bekker, Jacco C. Kromkamp, Hans C.P. Matthijs, and Klaas J. Hellingwerf. The redox potential of the plastoquinone pool of the cyanobacterium synechocystis species strain PCC 6803 is under strict homeostatic control. *Plant Physiology*, 165(1):463–475, 2014.

[58] Anita Santana-Sanchez, Daniel Solymosi, Henna Mustila, Luca Bersanini, Eva-Mari Aro, and Yagut Allahverdiyeva. Flavodiiron proteins 1–to-4 function in versatile combinations in O2 photoreduction in cyanobacteria. *eLife*, 8, 7 2019.

[59] Reza Ranjbar Choubeh, Emilie Wientjes, Paul C Struik, Diana Kirilovsky, and Herbert van Amerongen. State transitions in the cyanobacterium Synechococcus elongatus 7942 involve reversible quenching of the photosystem

II core. *Biochimica et Biophysica Acta (BBA) - Bioenergetics*, 1859(10):1059–1066, 10 2018.

[60] Ciaran R. McFarlane, Nita R. Shah, Burak V. Kabasakal, Blanca Echeverria, Charles A. R. Cotton, Doryen Bubeck, and James W. Murray. Structural basis of light-induced redox regulation in the Calvin–Benson cycle in cyanobacteria. *Proceedings of the National Academy of Sciences*, 116(42):20984–20990, 10 2019.

[61] Lauri Nikkanen, Daniel Solymosi, Martina Jokel, and Yagut Allahverdiyeva. Regulatory electron transport pathways of photosynthesis in cyanobacteria and microalgae: Recent advances and biotechnological prospects. *Physiologia Plantarum*, 173(2):514–525, 10 2021.

[62] Nina A Kamennaya, Seeun Ahn, Hanwool Park, Roy Bartal, Kenji A Sasaki, Hoi-Ying Holman, and Christer Jansson. Installing extra bicarbonate transporters in the cyanobacterium Synechocystis sp. PCC6803 enhances biomass production. *Metab. Eng.*, 29:76–85, 5 2015.

[63] Feiyan Liang and Peter Lindblad. Synechocystis PCC 6803 overexpressing RuBisCO grow faster with increased photosynthesis. *Metab Eng Commun*, 4:29–36, 6 2017.

[64] Xiang Gao, Fang Gao, Deng Liu, Hao Zhang, Xiaoqun Nie, and Chen Yang. Engineering the methylerythritol phosphate pathway in cyanobacteria for photosynthetic isoprene production from CO2. *Energy & Environmental Science*, 9(4):1400–1411, 2016.

[65] Masahiro Kanno, Austin L Carroll, and Shota Atsumi. Global metabolic rewiring for improved CO2 fixation and chemical production in cyanobacteria. *Nat. Commun.*, 8:14724, 3 2017.

[66] Amit K. Singh, María Santos-Merino, Jonathan K. Sakkos, Berkley J. Walker, and Daniel C Ducat. Multi-layer Regulation of Rubisco in Response to Altered Carbon Status in Synechococcus elongatus PCC 7942. *bioRxiv*, 10 2021.

[67] Marcel Grund, Torsten Jakob, Jörg Toepel, Andreas Schmid, Christian Wilhelm, and Bruno Bühler. Heterologous Lactate Synthesis in Synechocystis sp. Strain PCC 6803 Causes a Growth Condition-Dependent Carbon Sink Effect. *Appl. Environ. Microbiol.*, 88(8):e0006322, 4 2022.

[68] Alessandro Cordara, Angela Re, Cristina Pagliano, Pascal Van Alphen, Raffaele Pirone, Guido Saracco, Filipe Branco dos Santos, Klaas Hellingwerf, and Nicolò Vasile. Analysis of the light intensity dependence of the growth of Synechocystis and of the light distribution in a photobioreactor energized by 635 nm light. *PeerJ*, 6:e5256, 7 2018.

[69] Kiyan Shabestary, Hugo Pineda Hernández, Rui Miao, Emil Ljungqvist, Olivia Hallman, Emil Sporre, Filipe Branco dos Santos, and Elton P Hudson. Cycling between growth and production phases increases cyanobacteria bioproduction of lactate. *Metabolic Engineering*, 68:131–141, 11 2021.

[70] Melissa Cano, Steven C Holland, Juliana Artier, Rob L Burnap, Maria Ghirardi, John A Morgan, and Jianping Yu. Glycogen Synthesis and Metabolite Overflow Contribute to Energy Balancing in Cyanobacteria. *Cell Reports*, 23(3):667–672, 4 2018.

[71] Liat Adler, Aranzazú Díaz-Ramos, Yuwei Mao, Krzysztof Robin Pukacz, Chenyi Fei, and Alistair J McCormick. New horizons for building pyrenoid-based CO2-concentrating mechanisms in plants to improve yields. *Plant Physiology*, 190(3):1609–1627, 10 2022.

[72] Meng Li, Vaclav Svoboda, Geoffry Davis, David Kramer, Hans Henning Kunz, and Helmut Kirchhoff. Impact of ion fluxes across thylakoid membranes on photosynthetic electron

transport and photoprotection. *Nature Plants*, 7(7):979–988, 7 2021.

[73] Hui Lyu and Dušan Lazár. Analyzing the effect of ion binding to the membrane-surface on regulating the light-induced transthylakoid electric potential ($\Delta\Psi$m). *Frontiers in Plant Science*, 13, 7 2022.

[74] Laura Roxana Stingaciu, Hugh O'Neill, Michelle Liberton, Volker S. Urban, Himadri B. Pakrasi, and Michael Ohl. Revealing the Dynamics of Thylakoid Membranes in Living Cyanobacterial Cells. *Scientific Reports*, 6, 1 2016.

[75] Markus Janasch, Johannes Asplund-Samuelsson, Ralf Steuer, and Elton P Hudson. Kinetic modeling of the Calvin cycle identifies flux control and stable metabolomes in Synechocystis carbon fixation. *Journal of Experimental Botany*, 70(3):973–983, 2019.

[76] Gwenaëlle Moal and Bernard Lagoutte. Photoinduced electron transfer from photosystem I to NADP+: Characterization and tentative simulation of the in vivo environment. *Biochimica et Biophysica Acta (BBA) - Bioenergetics*, 1817(9):1635–1645, sep 2012.

[77] Nir Keren, Rajeev Aurora, and Himadri B. Pakrasi. Critical Roles of Bacterioferritins in Iron Storage and Proliferation of Cyanobacteria. *Plant Physiology*, 135(3):1666, 2004.

[78] Allison M.L. Van De Meene, William P. Sharp, Jennifer H. McDaniel, Heiner Friedrich, Wim F.J. Vermaas, and Robert W. Roberson. Gross morphological changes in thylakoid membrane structure are associated with photosystem I deletion in Synechocystis sp. PCC 6803. *Biochimica et Biophysica Acta (BBA) - Biomembranes*, 1818(5):1427–1434, may 2012.

[79] Martin Hagemann, Shanshan Song, and Eva-Maria Eva-Maria Brouwer. Inorganic Carbon Assimilation in Cyanobacteria: Mechanisms, Regulation, and Engineering. *Cyanobacteria Biotechnology*, pages 1–31, may 2021.

[80] Denys Pogoryelov, Christian Reichen, Adriana L. Klyszejko, René Brunisholz, Daniel J. Muller, Peter Dimroth, and Thomas Meier. The oligomeric state of c rings from cyanobacterial F-ATP synthases varies from 13 to 15. *Journal of bacteriology*, 189(16):5895–5902, aug 2007.

[81] Lijin Tian, Ivo H. M. van Stokkum, Rob B. M. Koehorst, Aniek Jongerius, Diana Kirilovsky, and Herbert van Amerongen. Site, Rate, and Mechanism of Photoprotective Quenching in Cyanobacteria. *Journal of the American Chemical Society*, 133(45):18304–18311, nov 2011.

[82] Andrew S. Richardson. *2019 NRL Plasma Formulary*. U.S. Naval Research Laboratory, 2019.

[83] Michael E. Wieser. Atomic weights of the elements 2005 (IUPAC Technical Report). *Pure and Applied Chemistry*, 78(11):2051–2066, jan 2006.

[84] Jocelyn Kauny and Pierre Sétif. NADPH fluorescence in the cyanobacterium Synechocystis sp. PCC 6803: A versatile probe for in vivo measurements of rates, yields and pools. *Biochimica et Biophysica Acta (BBA) - Bioenergetics*, 1837(6):792–801, jun 2014.

[85] Kenya Tanaka, Ginga Shimakawa, Hiro Tabata, Shoko Kusama, Chikahiro Miyake, and Shuji Nakanishi. Quantification of NAD(P)H in cyanobacterial cells by a phenol extraction method. *Photosynthesis Research*, 148(1):57, may 2021.

[86] Sofia Doello, Alexander Klotz, Alexander Makowka, Kirstin Gutekunst, and Karl Forchhammer. A Specific Glycogen Mobilization Strategy Enables Rapid Awakening of Dormant Cyanobacteria from Chlorosis. *Plant Physiology*, 177(2):594–603, jun 2018.

[87] Francisco Javier Mojica Prieto and Frank J. Millero. The values of pK1 + pK2 for the dissociation of carbonic acid in seawater. *Geochimica et Cosmochimica Acta*, 66(14):2529–2540, jul 2002.

[88] Paul G. Falkowski and John A. Raven. *Aquatic Photosynthesis*. Princeton University Press, jan 2007.

[89] Gábor Bernát, Nadine Waschewski, and Matthias Rögner. Towards efficient hydrogen production: The impact of antenna size and external factors on electron transport dynamics in Synechocystis PCC 6803. *Photosynthesis Research*, 99(3):205–216, 2009.

[90] Pierre Sétif, Ginga Shimakawa, Anja Krieger-Liszkay, and Chikahiro Miyake. Identification of the electron donor to flavodiiron proteins in Synechocystis sp. PCC 6803 by in vivo spectroscopy. *Biochimica et Biophysica Acta (BBA) - Bioenergetics*, 1861(10):148256, oct 2020.

[91] Maria Ermakova, Tuomas Huokko, Pierre Richaud, Luca Bersanini, Christopher J. Howe, David J. Lea-Smith, Gilles Peltier, and Yagut Allahverdiyeva. Distinguishing the Roles of Thylakoid Respiratory Terminal Oxidases in the Cyanobacterium Synechocystis sp. PCC 6803. *Plant Physiology*, 171(2):1307–1319, jun 2016.

[92] Shigeharu Kihara, Daniel A. Hartzler, and Sergei Savikhin. Oxygen concentration inside a functioning photosynthetic cell. *Biophysical Journal*, 106(9):1882–1889, may 2014.

[93] Tomáš Zavřel, Petra Očenášová, and Jan Červený. Phenotypic characterization of Synechocystis sp. PCC 6803 substrains reveals differences in sensitivity to abiotic stress. *PLoS ONE*, 12(12), dec 2017.

[94] Yonatan Savir, Elad Noor, Ron Milo, and Tsvi Tlusty. Cross-species analysis traces adaptation of Rubisco toward optimality in a low-dimensional landscape. *Proceedings of the National Academy of Sciences*, 107(8):3475–3480, feb 2010.

[95] Akira Wadano, Keisuke Nishikawa, Tomohiro Hirahashi, Ryohei Satoh, and Toshio Iwaki. Reaction mechanism of phosphoribulokinase from a cyanobacterium, Synechococcus PCC7942. *Photosynthesis Research*, 56(1):27–33, 1998.

[96] Yu Tsukamoto, Yuriko Fukushima, Satoshi Hara, and Toru Hisabori. Redox Control of the Activity of Phosphoglycerate Kinase in Synechocystis sp. PCC6803. *Plant and Cell Physiology*, 54(4):484–491, apr 2013.

[97] Olga Koksharova, Milada Schubert, Sergey Shestakov, and Rüdiger Cerff. Genetic and biochemical evidence for distinct key functions of two highly divergent GAPDH genes in catabolic and anabolic carbon flow of the cyanobacterium Synechocystis sp. PCC 6803. *Plant Molecular Biology*, 36:183, 1998.

[98] Jan Huege, Jan Goetze, Doreen Schwarz, Hermann Bauwe, Martin Hagemann, and Joachim Kopka. Modulation of the Major Paths of Carbon in Photorespiratory Mutants of Synechocystis. *PLOS ONE*, 6(1):e16278, 2011.

[99] Maximilian König, Jan Vaes, Elias Klemm, and Deepak Pant. Solvents and Supporting Electrolytes in the Electrocatalytic Reduction of CO2. *iScience*, 19:135–160, 9 2019.

[100] Ulrich Schreiber. Redox changes of ferredoxin, P700, and plastocyanin measured simultaneously in intact leaves. *Photosynthesis Research*, 134(3):343–360, dec 2017.

[101] Yuan-Hui Li and Tien-Fung Tsui. The solubility of CO 2 in water and sea water . *Journal of Geophysical Research*, 76(18):4203–4207, 1971.

[102] Hai Bo Jiang, Hui Min Cheng, Kun Shan Gao, and Bao Sheng Qiu. Inactivation of Ca2+/H+ exchanger in Synechocystis sp. strain PCC 6803 promotes cyanobacterial calcification by upregulating CO2-concentrating mechanisms. *Applied and Environmental Microbiology*, 79(13):4048–4055, jul 2013.

[103] J. Blunden and T. Boyer. State of the Climate in 2021. *Bulletin of the American Meteorological Society*, 103(8):S1–S465, aug 2022.

[104] Neil T. Miller, Michael D. Vaughn, and Robert L. Burnap. Electron flow through NDH-1 complexes is the major driver of cyclic electron flow-dependent proton pumping in cyanobacteria. *Biochimica et Biophysica Acta - Bioenergetics*, 1862(3), 3 2021.